Supplementary Information

References

1. **Dittmar KA, Sørensen MA, Elf J, Ehrenberg M, Pan T**. 2005. Selective charging of tRNA isoacceptors induced by amino-acid starvation. EMBO Rep **6**:151–157.

2. **Sørensen MA**. 2001. Charging levels of four tRNA species in Escherichia coli Rel+ and Rel- strains during amino acid starvation: a simple model for the effect of ppGpp on translational accuracy. J Mol Biol **307**:785–798.

3. **Pramanik J, Keasling J**. 1997. Stoichiometric model of Escherichia coli metabolism: incorporation of growth-rate dependent biomass composition and mechanistic energy requirements. Biotechnol Bioeng **56**:398–421.

4. **Bremer H, Dennis PP**. 1996. Modulation of chemical composition and other parameters of the cell by growth rate .

5. **Neidhardt FC, Umbarger HE**. 1996. Chemical composition of Escherichia coli .

6. **Mitarai N, Sneppen K, Pedersen S**. 2008. Ribosome collisions and translation efficiency: optimization by codon usage and mRNA destabilization. J Mol Biol **382**:236–245.

7. **Subramaniam AR, Zid BM, OShea EK**. 2014. An integrated approach reveals regulatory controls on bacterial translation elongation. Cell **159**:1200–1211.

8. **Moore SD, Sauer RT**. 2005. Ribosome rescue: tmRNA tagging activity and capacity in Escherichia coli. Mol Microbiol **58**:456–466.

9. **Parker J**. 1989. Errors and alternatives in reading the universal genetic code. Microbiol Mol Biol Rev **53**:273.

10. **Kubitschek H, Friske J**. 1986. Determination of bacterial cell volume with the Coulter Counter. J Bacteriol **168**:1466–1467.

11. **Murray DK, Bremer H**. 1996. Control of spoT-dependent ppGpp synthesis and degradation in Escherichia coli. J Mol Biol **259**:41–57.

12. **Pedersen S, Reeh S, Friesen JD**. 1978. Functional mRNA half lives in E. coli. Mol Gen Genet **166**:329–336.

13. **Pedersen M, Nissen S, Mitarai N, Svenningsen SL, Sneppen K, Pedersen S**. 2011. The functional half-life of an mRNA depends on the ribosome spacing in an early coding region. J Mol Biol **407**:35–44.

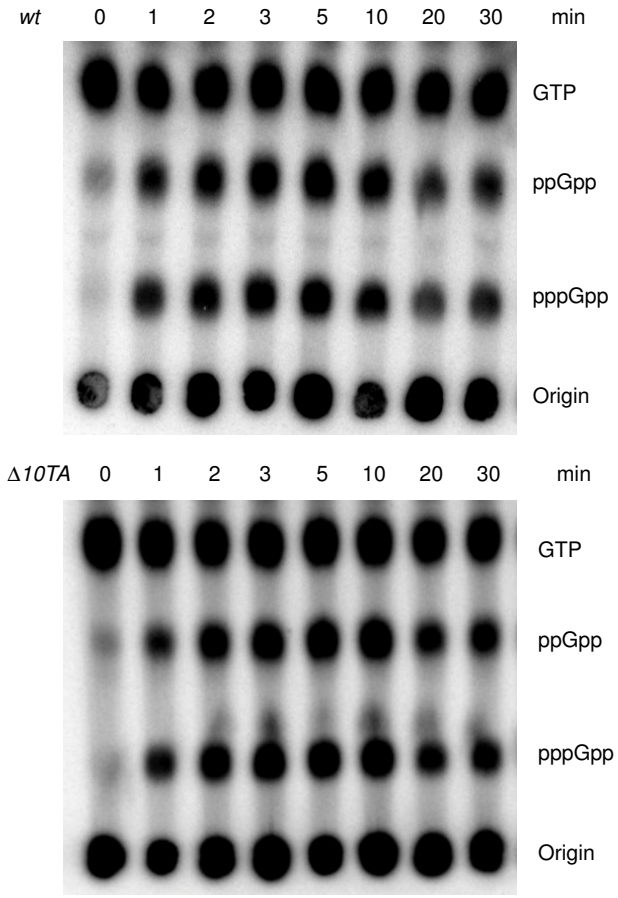

Figure S1. Representative audioradiogram of a PEI Cellulose TLC plate showing (p)ppGpp accumulation upon valine-induced isoleucine starvation (related to Fig. 1a). See Materials and Methods section for more details.

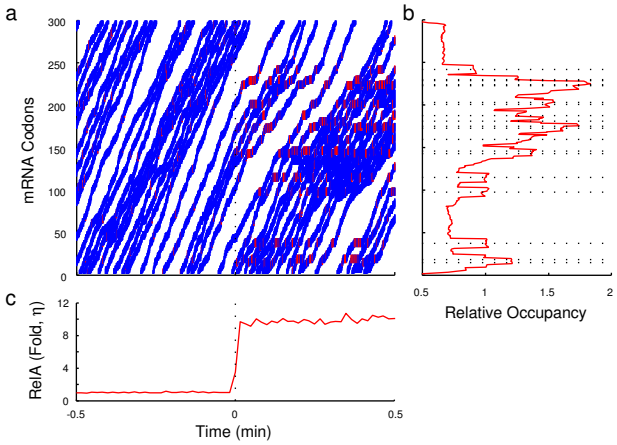

Figure S2. The ribosome trafficking model without abortion and mistranslation (related to Fig. 2). a. A spatiotemporal illustration of the ribosome traffic upon starvation. **b**. The relative occupancy of mRNA codons in the post-starved state. **c**. The relative RelA activity in the pre- and post-starved state.

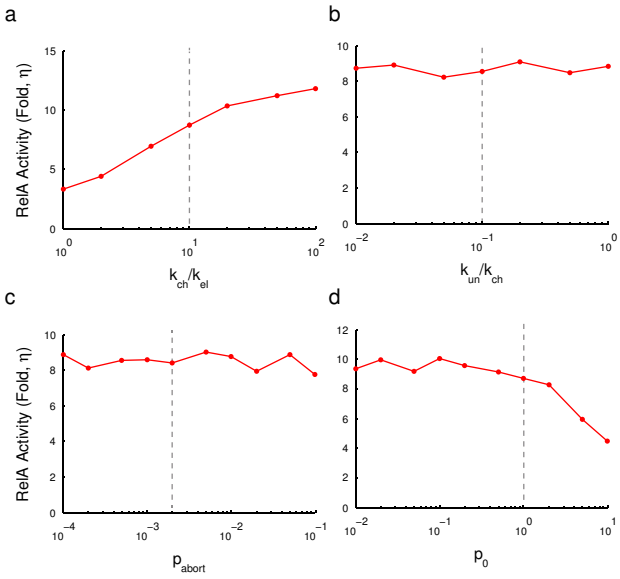

Figure S3. Sensitivity of the parameters in the ribosome trafficking model (related to Fig. 2). The steady state relative RelA activities in the post-starved states were measured for different values of **(a)** k_{ch}/k_{el}, **(b)** k_{un}/k_{ch}, **(c)** p_{abort} and **(d)** p_0. The dash lines represent the values used in the model (Table S1).

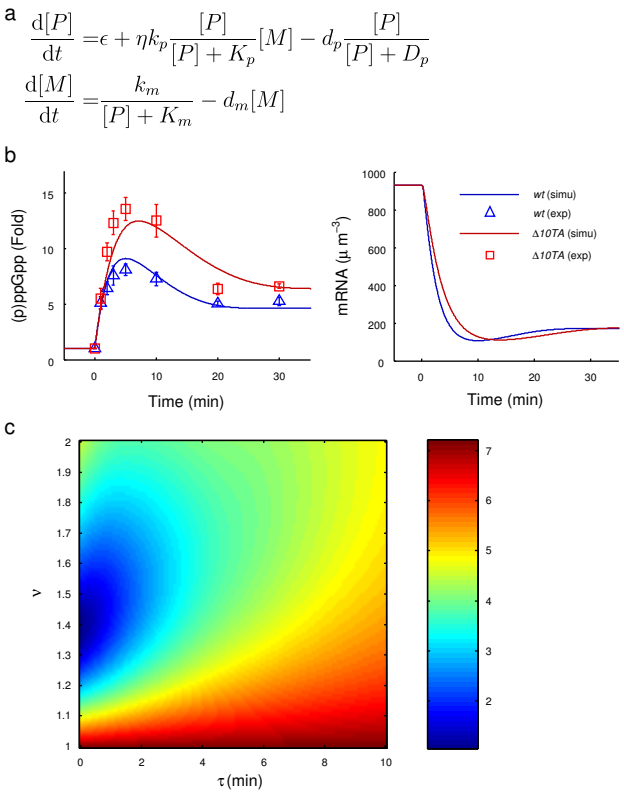

Figure S4. Model of early stringent response with both RelA- and SpoT-mediated positive feedbacks on ppGpp level (related to Fig. 3). **a**. The formulation of the model. **b**. The predicted concentrations of ppGpp (left) and mRNA (right) upon isoleucine starvation at $t = 0$. Blue curves represent the *wt* strain and red curves represent the $\Delta 10TA$ strain. Triangle (*wt*) and square ($\Delta 10TA$) symbols and the error bars are reproduced from Fig. 1a. **c**. The error of fitting to the *wt* measurements by modulating ν and τ. The method of error calculation is the same as Fig. 3d.

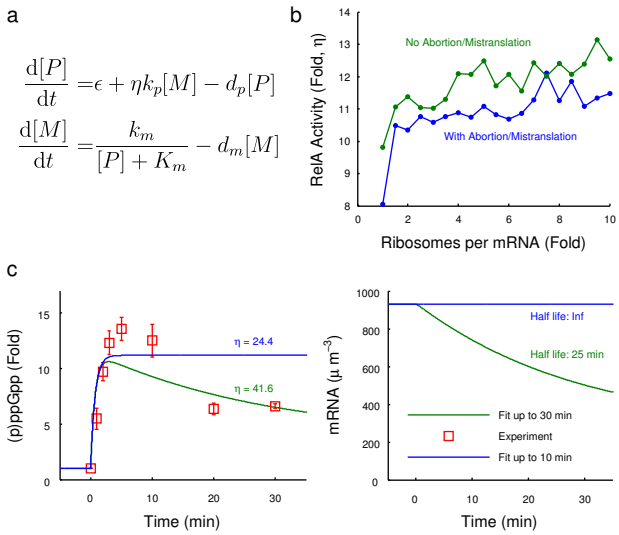

Figure S5. Model of early stringent response without positive feedbacks on ppGpp level (related to Fig. 3). a. The formulation of the model. **b**. The relative RelA activity in the post-starved state was measured in the ribosome trafficking models for multiple amount of ribosomes per mRNA to account for the transient reduction of mRNA level and the approximately constant ribosome level. The amount of ribosomes was expressed in the fold change to the pre-starved state (15, Table S1). The figure illustrates that with the parameter values listed in Table S1, the starvation signal could reach around 12-fold. The blue curve represents the ribosome trafficking model with abortion and mistranslation (related to Fig. 2) and the green curve represents the model without abortion and mistranslation (related to Fig. S2) **c**. The simulated concentrations of ppGpp and mRNA upon isoleucine starvation with the parameter values generated by the fitting algorithm (Materials and Methods). The green curves represent the fitting to the $\Delta 10TA$ data, and the blue curves represent the fitting to the the $\Delta 10TA$ data up to $t = 10$ min. Both fittings illustrate the necessity of a long mRNA half life. The square symbol and the error bars are reproduced from Fig. 1a.

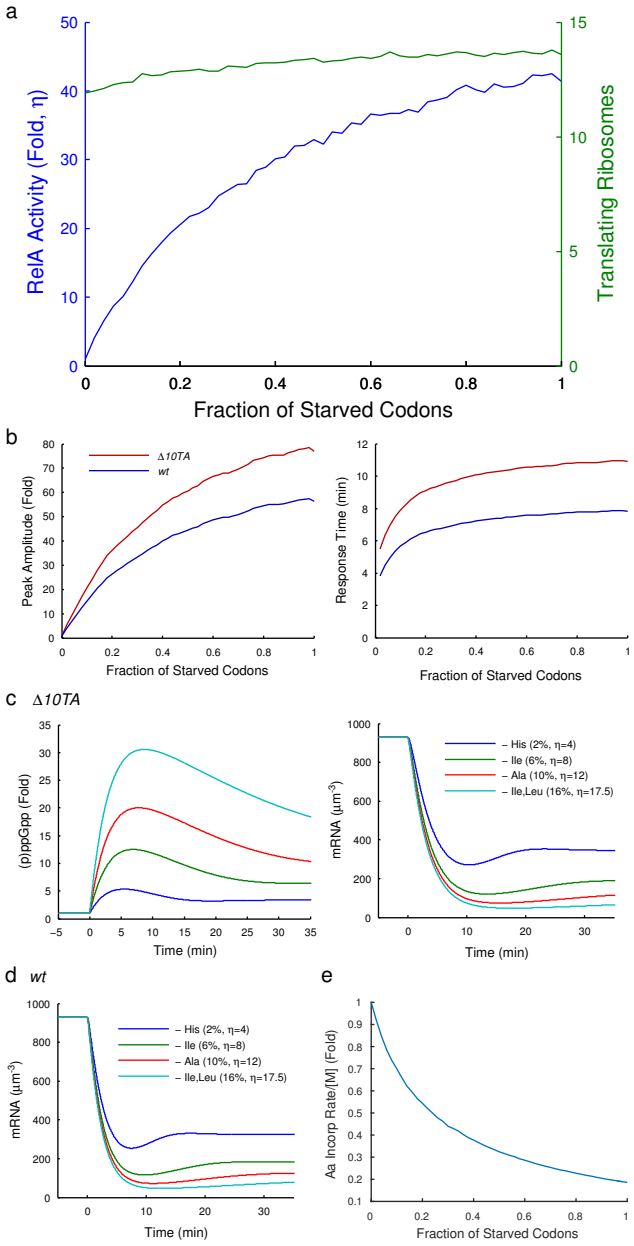

Figure S6. The predicted ppGpp response to general amino acid starvation (related to Fig. 4). **a**. The effect of the fraction of starved codons on the ribosome trafficking model. The blue curve represents the relative RelA activity (η) in the post-starved state to the pre-starved one, and the green curve represents the steady state number of translating ribosomes in the post-starved state. **b**. The amplitude (left) and the response time (right) were plotted as a function of the fraction of starved codons. **c**. The predicted levels of ppGpp (left) and mRNA (right) for the $\Delta 10TA$ strain. **d**. The predicted levels of mRNA for the *wt* strain (related to Fig. 4). **e**. The effect of the fraction of starved codons on the translation elongation rates, represented in the fold changes in the amino acid incorporation rate per mRNA in the post-starved state from the pre-starved one.

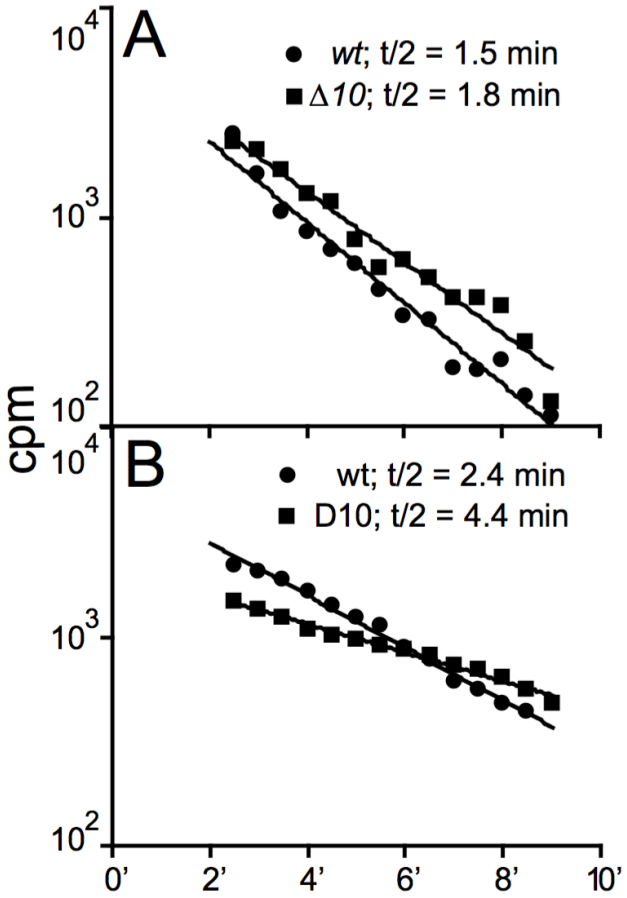

Figure S7. mRNAses reduce the global levels of mRNA stability during aa starvation. Global mRNA decay in *wt* and $\Delta 10TA$ strains was measured by following the loss of [^{3}H]uridine-incorporation into TCA-precipitable material (RNA) after addition of rifampicin, during steady state growth (**a**) and during aa starvation (**b**). Plotted is the time (min) after rifampicin addition vs. [^{3}H] incorporation shown as counts per minutes (cpm), see Materials and Methods for details.

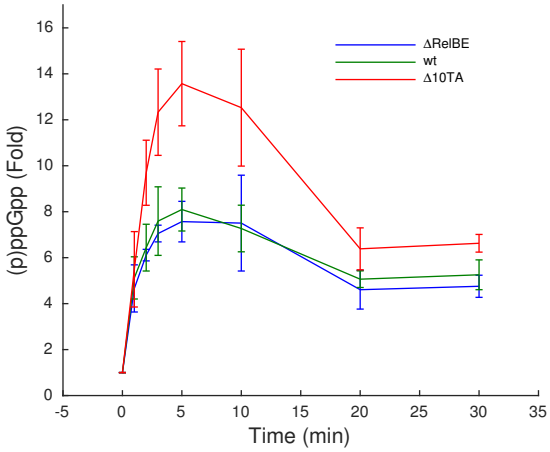

Figure S8. Early stringent response of $\Delta RelBE$ strain to isoleucine starvation. The levels of (p)ppGpp for the $\Delta RelBE$ strain were measured as described in Fig. 1 and Materials and Methods. The data points and error bars for wt and $\Delta 10TA$ strains were reproduced from Fig. 1.

Table S1. The parameter values in the ribosome trafficking model

Parameter	Meaning	Value	Remark
	The charging level of tRNA in the pre-starved state	0.8	[1, 2]
	The charging level of $tRNA^{Ile}$ upon isoleucine starvation	0.02	Ref. [2] measured that the charging level of $tRNA^{Leu}$ was between 1% and 3% upon leucine starvation. We assumed a similar value for isoleucine starvation due to the similarity in the amino acid structures.
	The usage of isoleucine in the proteins of *E.coli*	0.06	The usages listed in Ref. [3] after normalization.
	The copy number of ribosomes for translation	15	Ref. [4] measured that the copy number of ribosomes for *E.coli* with 60-minute double time is 1.35×10^4. The copy number of mRNA for *E.coli* with 40-minute doubling time is 1380 [5]. Note that the global synthesis rate of mRNA is 1.37×10^5 nucleotides per minute in cells with 40-minute doubling time and 9.2×10^4 for the cells with 60-minute doubling time. The copy number of mRNA in the 60-minute doubling cells is estimated to be $1380 \times (9.2 \times 10^4)/(1.37 \times 10^5) \approx 9.3 \times 10^2$, and the number of ribosomes per mRNA is $1.35 \times 10^4/(9.3 \times 10^2) \approx 15$.
	The number of codons a ribosome covers	11	[6]
k_{init}	The initiation rate of translation for a free ribosome	0.4 s^{-1}	Fitted to have around 80% ribosomes translating on the mRNA in the pre-starved states [4]
k_{ch}	The binding rate of charged cognate tRNA to the ribosomal A-site.	176 s^{-1}	The translation rate for *E.coli* with 60-minute doubling time is 16 codons per second [4] and the median time for the binding process takes around 10% of the overall elongation time [7]. So we set $k_{ch}/k_{el} = 10$. Combining with $1/k_{ch} + 1/k_{el} = 1/16$ s, one obtains that $k_{ch} = 176$ s^{-1} and $k_{el} = 17.6$ s^{-1}.
k_{el}	The rate of ribosomes elongating one codon	17.6 s^{-1}	
k_{un}	The binding rate of uncharged cognate tRNA to the ribosomal A-site.	17.6 s^{-1}	Assume to be 10-fold less than a charged cognate tRNA. Sensitivity analysis revealed that the parameter is insensitive to the relative RelA activity (Fig. S3).
p_{abort}	The abortion rate of translating ribosomes	0.002 s^{-1}	Fitted to have around 0.4% incomplete peptides in the pre-starved state [8]. This parameter is insensitive to the relative RelA activity (Fig. S3).
p_0	The parameter for calculating mistranslation (Materials and Methods)	1 s^{-1}	Fitted to have a mistranslation fraction of $5 * 10^{-3}$ in the pre-staved state, consistent with the previous reports [9]. A reduction in this parameter value will increase the RelA activity slightly (Fig. S3d) and the conclusions in the manuscript remain valid.

Table S2. The parameter values in the model of early stringent response with SpoT-mediated positive feedbacks

Parameter	Meaning	Value	Remark
$[P]_0$	Pre-starved level of ppGpp	$3.4 \times 10^4 \mu m^{-3}$	The level of ppGpp for cells with 60-minute doubling time is 38 pmol/OD_{460} and 1 OD_{460} corresponds to 6.7×10^8 cells [4]. We assume the size of E.coli cells to be 1 μm^3 with support from Ref. [10].
$[M]_0$	Pre-starved level of mRNA	$9.3 \times 10^2 \mu m^{-3}$	Table S1
ϵ	Basal production rate of ppGpp by SpoT	$4.0 \times 10^{-2} \mu m^{-3} s^{-1}$	Fitted
D_p	Michaelis-Menten constant for saturated degradation of ppGpp	$1.3 \times 10^4 \mu m^{-3}$	Fitted
K_m	Michaelis-Menten constant for transcriptional inhibition	$1.3 \times 10^4 \mu m^{-3}$	Fitted
k_p	Production rate of ppGpp by RelA	$4.2 \times 10^{-1} s^{-1}$	The level of ppGpp is in the steady state before starvation
d_p	The maximal degradation rate of ppGpp	$1.1 \times 10^3 \mu m^{-3} s^{-1}$	The half life of ppGpp in the pre-starved state is around 0.5 minute [11], so $d_p/([P]_0 + D_p) = ln(2)/30 s^{-1}$.
k_m	Transcription rate	$2.5 \times 10^5 \mu m^{-6} s^{-1}$	The level of mRNA is in the steady state before starvation
d_p	The half life of mRNA	$5.8 \times 10^{-3} s^{-1}$	The functional half life of mRNA is around 2 minutes [12, 13].
ν	The fold of reduction in the mRNA half life due to toxin's cleavage activity	1.4	Fitted
τ	The timescale for toxin release upon starvation	9.3 s	Fitted